

# An Overview of the Japanese GALA-V Wideband VLBI System

Mamoru Sekido<sup>1</sup>, Kazuhiro Takefuji<sup>1</sup>, Hideki Ujihara<sup>1</sup>, Tetsuro Kondo<sup>1</sup>, Masanori Tsutsumi<sup>1</sup>, Yuka Miyauchi<sup>1</sup>, Eiji Kawai<sup>1</sup>, Hiroshi Takiguchi<sup>1</sup>, Shingo Hasegawa<sup>1</sup>, Ryuichi Ichikawa<sup>1</sup>, Yasuhiro Koyama<sup>1</sup>, Yuko Hanado<sup>1</sup>, Ken-ichi Watabe<sup>2</sup>, Tomonari Suzuyama<sup>2</sup>, Jun-ichi Komuro<sup>1</sup>, Kenjiro Terada<sup>1</sup>, Kunitaka Namba<sup>1</sup>, Rumi Takahashi<sup>1</sup>, Yoshihiro Okamoto<sup>1</sup>, Tetsuro Aoki<sup>1</sup>, Takatoshi Ikeda<sup>1</sup>

**Abstract** NICT is developing a new broadband VLBI system, named GALA-V, with the aim of performing frequency comparisons between atomic time standards over intercontinental baselines. The development of the broadband GALA-V system is coordinated to be as compatible as possible with the VGOS system. Two types of original broadband feed systems were developed for the Kashima 34-m antenna of modified Cassegrain optics. The first prototype feed, called IGUANA-H, works in the 6.5–16 GHz frequency range, while the second feed, NINJA, works in the 3.2–14 GHz range. The GALA-V observation system is designed to capture four bands of 1024 MHz width in the 3–14 GHz range. Two types of data acquisition modes are available. One is a narrow channel mode, which acquires multiple channels with 32-MHz bandwidth. This mode is compatible with the NASA Proof-of-Concept (PoC) system developed by MIT Haystack Observatory. The other is a broad channel acquisition mode, in which a signal of 1024 MHz width is digitized as a single channel. A radio frequency (RF) direct sampling technique was used in this mode as a new approach for broadband observation taking advantage of the high-speed sampler K6/GALAS and its digital filtering function. This technique has several advantages in the precise delay measurement of the broadband bandwidth synthesis. VLBI experiments were conducted between the Kashima 34-m antenna and the Ishioka 13-m VGOS station of GSI, Japan. The first broadband observation over 8-GHz bandwidth was successful on this baseline in early 2015. The

results of the broadband bandwidth synthesis over 8-GHz bandwidth proved sub-pico-second resolution group delay measurement with one second of integration time. Time series of the group delay data showed several picoseconds of fluctuation over a few hundred seconds of time. The Allan standard deviation is consistent with the frozen flow model of Kolmogorov tropospheric turbulence.

**Keywords** GALA-V, broadband VLBI

## 1 Introduction

The time interval of the SI second as time scale is defined by counting the microwave emission from Cs atom at 9,192,631,770 Hz. Recent technological progress in quantum physics and optics allows to realize more accurate frequency standards by using optical emission of atoms [1]. A re-definition of the time scale has been discussed as a subject in metrology [2]. NICT is charged as a national institute with keeping Japan Standard Time and is engaged in research and development of optical frequency standards. A confirmation of the identity of the frequency generated by independent optical atomic standards is an important subject for a re-definition of the SI second.

Currently two-way satellite time and frequency transfer (TWSTFT) and observation of GNSS satellites are operationally used for distant frequency transfer. Advanced TWSTFT technology with carrier-phase [3] might provide enough precision over inter-continental distances, but it depends on the availability of satellite transponders. VLBI has the potential to enable distant

1. National Institute of Information and Communications Technology

2. National Institute of Advanced Industrial Science and Technology, National Metrology Institute of Japan

frequency transfer, which has been investigated in several studies [4]–[9]. One of the advantages of VLBI is that it is independent of the availability of satellites. The development of a more precise VLBI observation technology is in progress, and it is expected to advance the VLBI application in geodesy and metrology.

The IVS is promoting the deployment of VGOS as the new generation geodetic VLBI system. The VGOS system is characterized by a high temporal resolution of the observations by using fast slewing antennas and a broad radio frequency bandwidth. The fast source switching is necessary for VGOS to improve on the correct atmospheric delay modeling and its temporal resolution. The VLBI group at NICT is developing a broadband VLBI system named GALA-V in order to apply the VLBI technique to distant frequency transfer. The GALA-V system is basically designed to use a compatible radio observation frequency range as well as data acquisition system with the VGOS. The concept of the GALA-V system and the development of an original feed and data acquisition system are described in Section 2. Domestic broadband VLBI experiments between Kashima 34-m and the Ishioka 13-m VGOS station were conducted in 2015. The observation conditions and the derived broadband delay are discussed in Section 3. Finally, in Section 4 we summarize the overall progress.

## 2 Broadband VLBI System: GALA-V

### 2.1 Distant Clock Comparison with Small Antennas

A frequency comparison with VLBI is made by clock parameter estimation just as with geodesy. The standard signal from the atomic frequency standard is used as reference for the VLBI observations at each station; thus, the VLBI delay observable on that baseline contains the difference between those atomic clocks. To utilize VLBI for atomic frequency transfer, the VLBI stations need to be located near the atomic frequency standard, except for the case that the reference signal comes from a remote atomic clock via a stable fiber link (e.g., [10]). Thus our GALA-V system uses transportable small VLBI stations as the terminal of the comparison. Figure 1 shows the concept of the

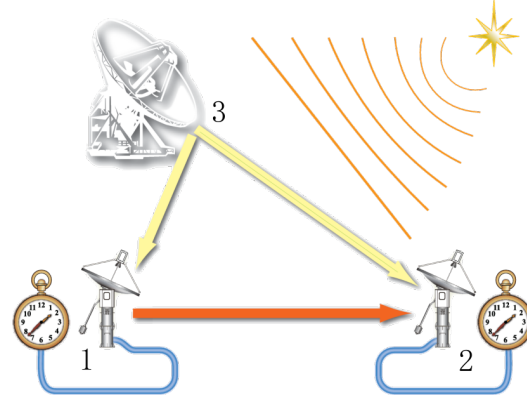


Fig. 1 Concept of the GALA-V broadband VLBI system.

GALA-V broadband VLBI system. The GALA-V observation system can be characterized by the following:

1. High-speed sampling: 1 GHz  $\times$  4 bands, 8 Gbps per polarization.
2. Combination use of small antennas with a large diameter antenna.
3. Non-redundancy array of observation frequency allocation to get a fine delay resolution function.
4. Broadband observation: 3–14 GHz.
5. RF direct sampling without frequency conversion.

The disadvantage of the lower sensitivity due to the small collecting area is mitigated by using (1) broadband observations and (2) the combination observation with a large-diameter antenna. The data acquisition rate of the GALA-V system is 8192 Mbps corresponding to 4  $\times$  1-GHz bands, whereas the conventional geodetic VLBI observation uses about 256 Mbps. GALA-V brings about a 5.6 ( $=\sqrt{8192/256}$ ) times improvement in SNR when compared to conventional VLBI. The signal-to-noise ratio of the VLBI observation is expressed by the product of the system equivalent flux densities (SEFD) of two stations as

$$SNR = \frac{S}{SEFD_1 \cdot SEFD_2} \sqrt{2Bt}, \quad (1)$$

where  $S$  is the flux of the radio source,  $B$  is the observation bandwidth, and  $t$  is the integration time. Thus, even if the SNR of the VLBI observation with a pair of small antennas ‘1’+‘2’ is not sufficient for reaching a target SNR, the joint observation with the large-diameter (boost) antenna ‘3’ enables the interferometer to work. The delay observable of the baseline  $\tau_{21}(t_1)$  is computed by combining the two observables  $\tau_{13}$  and

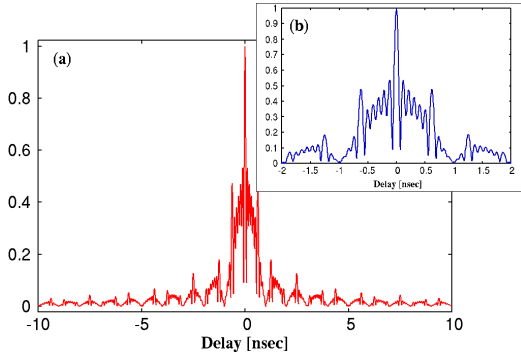


**Fig. 2** (a) Delay resolution function as expected from the frequency array at 4.0 GHz, 5.6 GHz, 10.4 GHz, and 13.6 GHz with 1-GHz bandwidth and (b) a magnified plot around the center.

$\tau_{23}$  and using the closure delay relation as follows:

$$\tau_{21}(t_1) = \tau_{23}(t_3) - \tau_{13}(t_3) - \tau_{13} \times \dot{\tau}_{21} + \frac{1}{2} \tau_{13}^2 \times \ddot{\tau}_{21} + o_3, \quad (2)$$

assuming that radio source structure effect is negligible. Although the error of the observable  $\tau_{12}$  increases by the root-square sum of the errors  $\tau_{23}$  and  $\tau_{13}$ , the advantage of this method is that systematic errors caused by the boost station cancel out. The radio source structure effect in the broadband observation is a subject of investigation.

After a local survey of the radio interference environment, we selected the nominal frequency array of the GALA-V system at 4.0 GHz, 5.6 GHz, 10.4 GHz, and 13.6 GHz for the center frequencies of the observation bands. By allocating the array in a non-redundancy interval, the delay resolution function has a fine peak and low side-lobes as indicated in Figure 2.

‘RF Direct Sampling’ is our original approach to enable easily do the broadband phase calibration by observation of a radio source. A stable phase relation between the observing bands is a prominent feature of this method. More details of this technique are described in Section 2.3.

It is well known that the atmospheric delay is the dominating error source with space-geodetic techniques including VLBI. For that a fast source switching is essential to improve the precision of both the geodetic results and the distant clock comparison. Therefore, the GALA-V project expects to make joint VLBI observations with a VGOS station as boost station in order to improve both the SNR and the temporal resolution.

## 2.2 Broadband Feed Development

The GALA-V system is designed to have a common radio observation frequency range with VGOS for joint observations. Most of the VGOS stations use the Eleven Feed [11] or the Quad-ridged Flared Horn (QRFH) [12] to receive the broadband radio signal. These feeds have a broader beam size at around 90–120°. Therefore, all new VGOS antennas are of the special optics design called “ring focus” in order to adapt to the broad beam size.

Using a different approach, we developed an original broadband feed with narrow beam size (34°) for the Cassegrain optics of the Kashima 34-m antenna. The first prototype feed “IGUANA-H” was produced in 2014. The design was based on a multi-mode wave composition, and it works at the frequency range 6.5–16 GHz. The second prototype feed “NINJA” was mounted on the 34-m antenna in 2015. It is sensitive in the frequency range 3.2–14 GHz.

Figure 3a shows the broadband receiver system of the Kashima 34-m antenna. The left hand side of the picture is the NINJA feed, the right hand side shows the IGUANA-H feed. The frequency dependence of the SEFDs of each feed is indicated in Figures 3b and 3c.

## 2.3 RF Direct Sampling with K6/GALAS(OCTAD-G)

The current standard VGOS observation system is based on the Proof-of-Concept (PoC) VLBI system developed at MIT Haystack Observatory [13, 14]. This system uses UpDown converters (UDC) for selecting four bands of 1-GHz bandwidth in the 2–14 GHz range. The signals are converted to intermediate frequencies (IF) in 32 channels of 32-MHz bandwidth using digital baseband conversion (DBBC, e.g., [15]–[17]) for each band. The phase relation among the 32 video channels must be stable, because each video frequency channel is separated in the digital signal processing after the IF signal is converted to digital data. The phase relations between the selected four bands using the UDC are not always constant; they may change and could even be sensitive to temperature mainly because of the analog mixing components and the local oscillators for each band. The concept

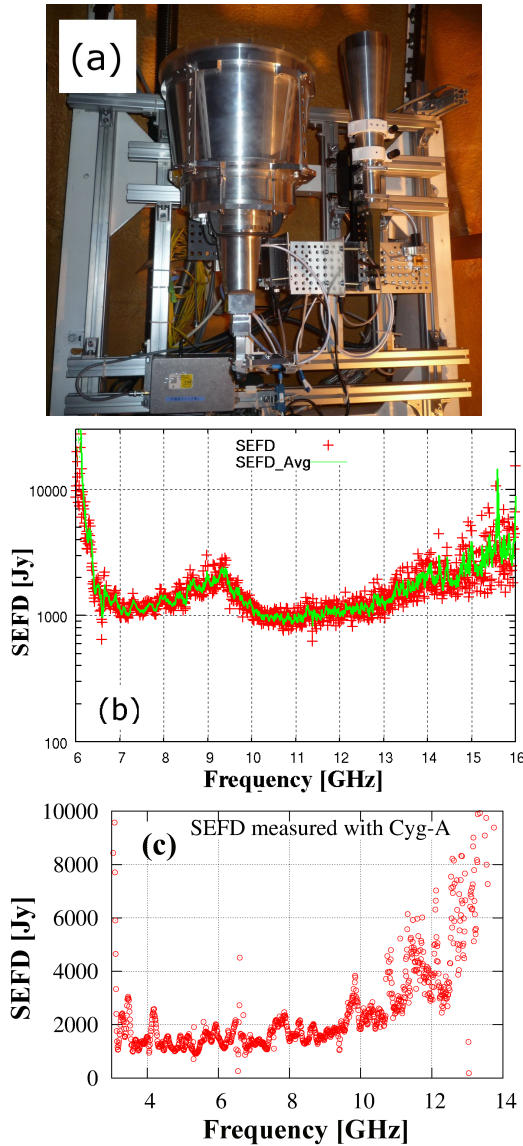


**Fig. 3** Picture (a) of the NINJA (left) and IGUANA-H (right) feeds and SEFDs of the IGUANA-H (b) and NINJA (c) feeds.

of VGOS aims at deriving the so-called ‘broadband delay’ [18] from the coherent synthesis of the fringe phase over the four bands. The phase calibration signal, which is injected into the signal path at the front end and later digitally recorded, is essential for calibrating the phase variation.

Our GALA-V system takes a different approach: sampling the radio frequency (RF) signal without analog frequency conversion, an ‘RF Direct Sampling’ technique [19]. This technique was enabled by the 16-

**Table 1** K6/GALAS Sampler specification parameters.

Input	
Number of inputs	2
Input freq. range	0.1–16.4 GHz
Sampling rate	16,384 MHz or 12,800 MHz
Quantization bit	3 bit
Output	
Sampling mode	Broadband mode
	3200 Msps: 1, 2 bit
	6400 Msps: 1, 2 bit
	12800 Msps: 1 bit
	DBBC mode
	LO resolution of frequency is 1 MHz.
	Nch: 1, 2, 3, 4
	Sample rate: 2048 Msps
	Quantization bit: 1 or 2 bit
Max data rate/sampler	16,384 Mbps
Output interface port	10GBASE-SR (SFP+), 4 ports
Data format	VDIF/VTP over UDP/IP
Control	Telnet /1000BaseT

GHz, high-speed sampler K6/GALAS (OCTAD-G). An image of this sampler is displayed in Figure 4a. The National Astronomical Observatory of Japan (NAOJ) and Elecs Co Ltd have been developing a series of a VLBI observation system called OCTAVE [20]. The high-speed sampler OCTAD is a member of the OCTAVE family with a 3-bit quantization at a 8,192 MHz sampling rate. The K6/GALAS is an upgraded version of OCTAD; this sampler realizes the analog-digital (A/D) conversion at a 16,384 MHz sampling rate with a 3-bit quantization. Then digital filtering via internal FPGA is applied to extract the 1024-MHz bandwidth signal at the requested frequency. The nominal observing mode is 2048 Msps-1bit-4band; the observed data come out at a data rate of 8,192 Mbps via the 10 GBASE-SR port with VDIF/VTP protocol as UDP/IP data stream.

A block diagram of the signal input to the sampler is shown in Figure 4b. The power divider and anti-aliasing filters have to be used to eliminate folding of the signal at 8,192 MHz. Then the signal is fed to two RF input ports to obtain four 1024-MHz bands distributed over the 3–14 GHz frequency range. Since the dynamic range of the A/D conversion at the input is limited, the input power level needs to be equalized over the broad frequency range. The data acquisition parameters and interface specifications of the K6/GALAS sampler are summarized in Table 1.

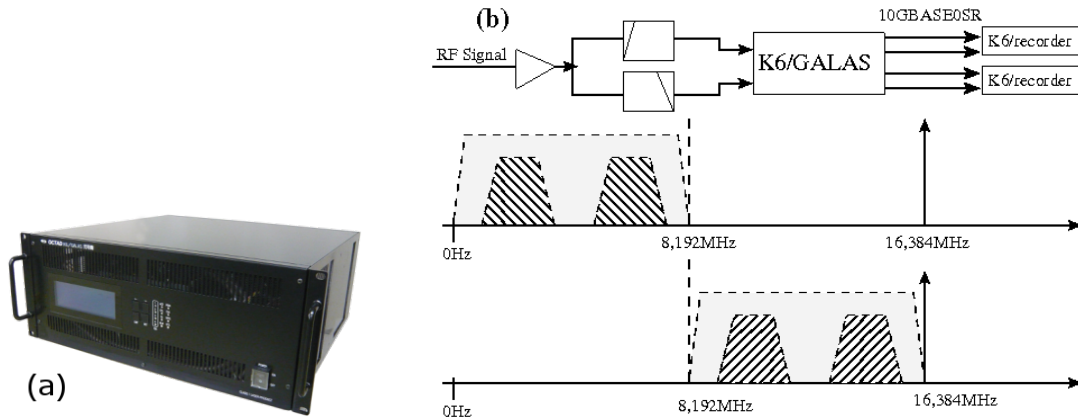


**Fig. 4** (a) Picture of the K6/Galas sampler. (b) Block diagram from sampler input to data recording. Two anti-alias filters are used to eliminate folding of the signal at a sampling rate of 16,384 MHz.

## 2.4 Wideband Bandwidth Synthesis without Pcal Signal

A prominent feature of the ‘RF Direct Sampling’ is its stable phase relation that enables broadband bandwidth synthesis without a phase calibration (Pcal) signal. The phase calibration technique with Pcal signal has been used since the 1980’s [21] to utilize the invention of bandwidth synthesis [22]. The most significant phase change in the signal chain of the observation system happens during frequency conversion. It is unavoidable that the local oscillator’s initial phase is included in the converted signal. Consequently, large phase differences between signals happen naturally. The Pcal signal has effectively corrected phase differences in the signal chain of multi-channel VLBI systems (e.g., [21, 23]). The frequency range to be synthesized has been up to 1-GHz width in the conventional VLBI system, whereas with VGOS and GALA-V the bandwidth to be synthesized is about ten times wider than the conventional VLBI. The broadband phase calibration is an essential technology to achieve such high delay resolution; hence, the broadband Pcal signal has to be quite stable.

The ‘RF Direct Sampling’ technique enables broadband phase calibration without a Pcal signal. The observed signal is converted to digital data in the radio frequency region without frequency conversion; the phase relation of the signal is conserved at this point. The required frequency bands are extracted via digital signal processing in the following step. Since frequency conversion is a major cause for inserting

phase differences between bands, we can expect that the phase relation over the captured broad frequency range will be stable enough to eliminate the need for calibration with Pcal signal.

A wideband bandwidth synthesis algorithm (WBWS) [24] is being developed, in which the band-pass cross spectrum phase for a strong radio source is used to perform the broadband phase calibration. The WBWS estimates the ionospheric dispersive delay and the broadband group delay simultaneously. Instead of using a Pcal signal, the WBWS method requires a ‘calibration scan’ (CalScan) within a VLBI session. The CalScan is an observation of a compact strong radio source with relatively long duration to get a sufficiently small phase error in the cross correlation spectrum. Since the CalScan cross correlation phase data contains not only the instrumental delay, but also the geometrical, ionospheric, and atmospheric propagation delays of the scan, the user has to be aware that the group delay obtained by the WBWS is a differential delay with respect to the CalScan.

## 3 Broadband VLBI Experiment and Delay Variation

### 3.1 Kashima–Ishioka Experiment

The Geospatial Information Authority of Japan (GSI) has constructed a new 13.2-m diameter VLBI station [25] at Ishioka city in Japan. The Ishioka station



**Table 2** Observation parameters of the broadband VLBI experiment in August 2015 on the Kashima 34-m – Ishioka 13-m baseline.

<b>Date and Duration</b>	2015y226d06h40m – 227d14h59m (32h20m),
<b>Scan</b>	2 scans of 1200 seconds and 1188 scans of 30 seconds
<b>Frequency Array [MHz]</b>	3200–4224, 4600–5624, 8800–9824, 11600–12624
<b>Effective bandwidth</b>	3.3 GHz
<b>Data Acquisition</b>	K6/GALAS & K6/recorder
<b>Data Acquisition Mode</b>	2048Mps-1bit-4band
<b>Polarization</b>	Vertical – Vertical

is fully compliant with the VGOS specifications. Thus Kashima 34-m of NICT and Ishioka 13-m of GSI are the only two stations in Japan with a broadband receiver system with an SEFD better than 2000 Jy. In collaboration with GSI, we have installed K6/GALAS DAS at Ishioka in August 2015. A test VLBI experiment in the observation frequency range of 3.2–12.6 GHz was conducted on this baseline. The observation parameters of this experiment are listed in Table 2.

Only one linear polarization was available with the NINJA feed of the Kashima 34-m station at the time. As the baseline between Ishioka 13-m and Kashima 34-m is very short (48.6 km), the parallactic angle of the polarization is negligible. The observation was done with one vertical linear polarization at both stations. The experiment included two long scans (1,200 s) and many short scans (30 s) in the more than 24 hours. The reasons for the long scans were twofold: examining the broadband delay behavior in the experiment and obtaining CalScan data for the WBWS processing. The cross correlation processing was done by the software correlator GICO3 [26] for each band. Finally, the post-correlation data were processed with the upgraded bandwidth synthesis software ‘komb’ (Ver. 2015-4-27) [24].

The process of WBWS includes the estimation of the dispersive delay and the broadband group delay. The cross spectrum phase is modeled by

$$\phi_{\text{meas}}(f) = \alpha \frac{\delta \text{TEC}}{f^2} + \delta \tau_a + \phi_o, \quad (3)$$

where the first term on the right hand side is the dispersive delay corresponding to the difference of the total electron content ( $\delta \text{TEC}$ ) in the lines-of-sight from each observation station, and the second term is the non-dispersive delay including the geometrical delay and the tropospheric delay. Figure 5a shows the cross spectrum phase and 5b shows the time series of estimated

$\delta \text{TEC}$ . Let me remind the reader that these data are differential quantities with respect to the CalScan used in the process. It is notable that up to several TECU<sup>1</sup> of dispersive delay contribution exist even on the short 48.6-km baseline.

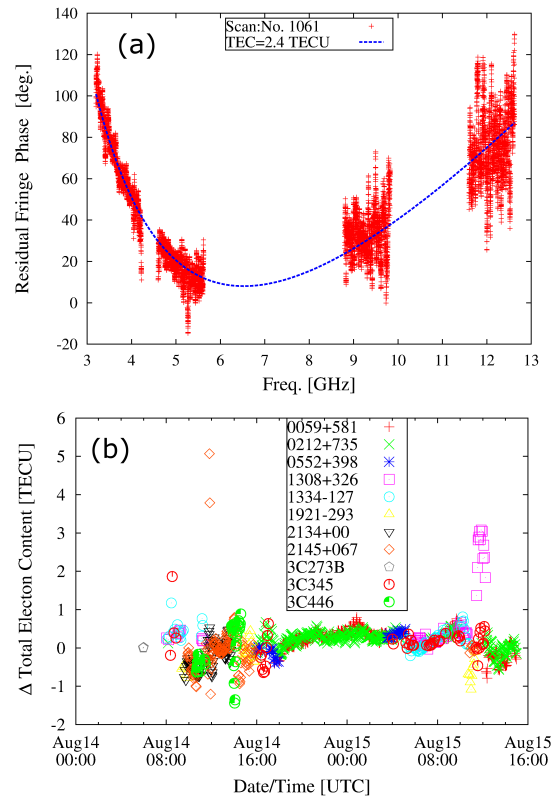


**Fig. 5** (a) An example of the cross correlation phase spectrum. The dashed line is a plot of Equation (4) with parameters fitted to the data. (b) Time series of the estimated  $\delta \text{TEC}$  obtained in the experiment. Each symbol corresponds to one radio source.

<sup>1</sup> 1 TECU =  $10^{16}$  electrons/m<sup>2</sup>

### 3.2 Broadband Delay

Figure 6a shows a time series of the group delay data of one-second integration after removal of a second-order polynomial for the slow delay change, and its Allan standard deviation (ASD) is displayed in Figure 6b. That scan was about 1,000 seconds long observing source 3C273B. The plot of the ASD indicates that the broadband delay of this case (effective bandwidth 3.3 GHz) reaches sub-pico-second precision at one-second observation when strong radio sources are observed.

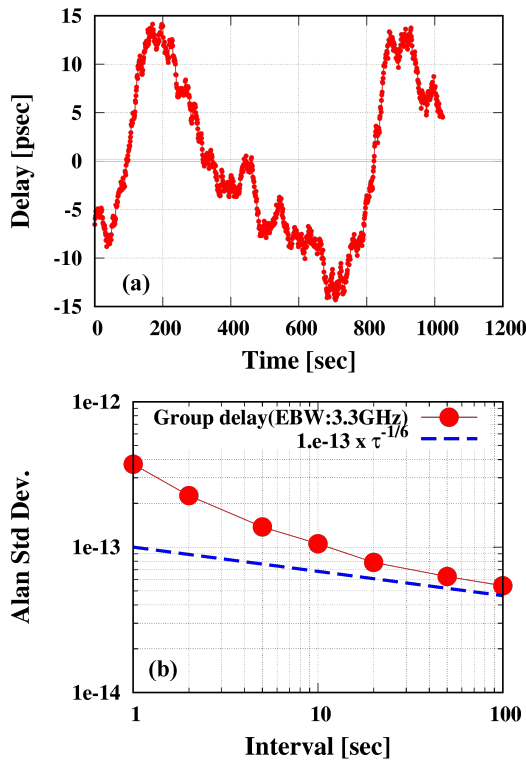


**Fig. 6** (a) Time series of group delay data derived by WBWS after removal of a second order polynomial for the slow delay change. (b) Allan standard deviation of the delay data. The dashed line is a plot of  $\sigma_y = 10^{-13} \tau^{-1/6}$ .

It is notable that the group delay change on the order of ten picoseconds over hundreds of seconds of time was observed with a very high precision. There are several candidate causes which can affect the group delay variation: troposphere propagation excess delay, instrumental delay, radio source structure effect, ionospheric delay, and model error of the geometrical de-

lay. A model error of the geometrical delay will cause a slow variation related to Earth rotation. Also, the radio source structure effect will change the group delay with the rotation of the projected baseline with respect to the source. Thus, these two are unlikely to be the reason for the short time variation. A rapid change of the ionospheric delay may be caused by traveling ionospheric disturbances (TID, e.g., [27]), which is 100 km scale with order of 1 TECU amplitude traveling with velocity around 400 km/hour. Its time scale is about 1,000 seconds, then it seems to be too long to explain this variation. The tropospheric delay is known to be the dominating error source in space-geodetic observations. The Allan variance of the tropospheric delay in interferometric observations is modeled by the frozen flow of the Kolmogorov turbulence [28].

$$\sigma_y^2(\tau) = 1.3 \times 10^{-17} C_n^2 L v_s^{5/3} \tau^{-1/3}, \quad (4)$$

where  $C_n^2 L$  is the constant of the turbulence,  $v_s$  is the wind velocity on the ground surface in m/s, and  $\tau$  is the time interval. Armstrong and Sramek [29] have measured  $C_n^2 L$  as  $2 \times 10^{-13} \sim 2 \times 10^{-9}$  for a 35 km spatial scale. By using wind speed (4 m/s) measured on the ground at the time of observation, the ASD can be computed as  $4.8 \times 10^{-13} \sim 2 \times 10^{-15}$  at  $\tau = 1$  second interval. Figure 6b shows the ASD derived from the time series of the group delay and plot of  $\sigma_y(\tau) = 10^{-13} \tau^{-1/6}$ . This good agreement between measurement and model in both slope and magnitude of ASD suggests that the delay fluctuation may be attributed to tropospheric turbulence.

The baseline analysis was made with CALC/SOLVE [30] for this broadband VLBI experiment. Although the delay precision is better than one picosecond for each data point, the root mean square (RMS) of the post-fit delay residual after standard parameter estimation was 34 picoseconds with a large Chi-square value. That means that the scattering of the residuals cannot be explained by the magnitude of the delay error computed from the SNR and bandwidth. Re-weighting of the data with additive noise of 55 picoseconds reduced Chi-square to unity. This result suggests that an unmodeled error dominates the errors of the VLBI analysis, and that this is likely the tropospheric delay as suggested by the delay fluctuation data. The formal errors of the station coordinates in the final solution were 3–4 mm in the horizontal and 1.3 mm in the vertical direction.

## 4 Summary

NICT is developing a wideband VLBI system (GALA-V) for frequency transfer over long distances. The observed radio frequency range is compatible with the VGOS specifications. To enable broadband observations with the Kashima 34-m radio telescope of Cassegrain optics, two types of original broadband feeds named IGUANA-H (6.5–16 GHz) and NINJA (3.2–14 GHz) were developed. A new high-speed sampler K6/GALAS was introduced for using the ‘RF Direct Sampling’ technique. An outstanding feature of ‘RF Direct Sampling’ is the stable phase relation between the bands selected by digital filtering. Since the signal path is simple and the data is digitized in an early stage, a high stability in phase and path length of the signal can be anticipated. The broadband delay is derived by the WBWS processing via phase calibration with a radio source signal (CalScan).

We have conducted a broadband VLBI experiment between the Kashima 34-m antenna and the Ishioka 13-m station, which is the only fully VGOS compliant station in Japan built by GSI in 2014. The experiment was composed of a geodetic session with 1,188 scans of 30 seconds in duration and two scans of long 1,200 seconds in duration. The cross correlation processing was done with the software correlator GICO3. The phase characteristic of the post-correlation data of whole bandwidth was calibrated with the phase data of a reference radio source (CalScan). Then the broadband group delay and the dispersive  $\delta\text{TEC}$  were simultaneously estimated in the WBWS process. The experiment has proven that the broadband delay enables sub-pico-second precision group delay measurements with one-second integration time. The behavior of the delay observable shows a fluctuation, which is consistent with the frozen flow model of the Kolmogorov tropospheric turbulence.

## Acknowledgements

We express our gratitude to Yoshihiro Fukuzaki, Ry-oji Kawabata, and Takahiro Wakasugi of GSI Japan for the collaboration in the joint observation with Ishioka 13-m station. We thank the “New Generation Network Testbed JGN-X” for supporting our project by providing a 10-Gbps network environment.

## References

1. B. J. Bloom et al., “An optical lattice clock with accuracy and stability at the  $10^{-18}$  level”, *Nature*, 506, DOI 10.1038/nature12941, 71–77, 2014.
2. J. Guèna et al., “Contributing to TAI with a secondary representation of the SI second”, *Metrologia*, 51(1), DOI 10.1088/0026-1394/51/1/108, pages 108–120, 2014.
3. M. Fujieda et al., “Carrier-Phase-Based Two-Way Satellite Time and Frequency Transfer”, *IEEE Ultrason. Ferroelectr. Freq. Control*, 59(12), DOI 10.1109/TUFFC.2012.2503, pages 2625–2630, 2012.
4. R. J. Coates and Clark, T. A., “Worldwide time and frequency synchronization by planned VLBI networks”, *In Its Proc. of the Sixth Ann. Precise Time and Time Interval (PTTI) Planning Meeting*, pages 361–371, 1974.
5. S. Hama et al., “First international Time and Frequency Comparison Experiment by using Very Long Baseline Interferometry”, *J. Radio Res. Lab.*, 34(142), 85–93, 1987.
6. H. Takiguchi et al., “VLBI Measurements for Frequency Transfer”, *Highlights of Astronomy*, Vol.15, Proc. of XXVIIIth IAU General Assembly in August 2009, DOI 10.1017/S1743921310008926, pages 225, 2010.
7. C. Rieck et al., “VLBI time-transfer using CONT08 data” *EFTF-2010 24th European Frequency and Time Forum*, DOI 10.1109/EFTF.2010.6533654, pages 1–8, 2010.
8. R. Haas et al., “VLBI and GNSS Frequency Link Instabilities during CONT Campaigns”, *IVS 2012 General Meeting Proceedings* Edited by Dirk Behrend and Karen D. Baver NASA/CP-2012-217504, pages 425–430, 2012.
9. C. Rieck et al., “VLBI Frequency Transfer using CONT11”, *Proc. of European Frequency and Time Forum (EFTF) 2012*, DOI 10.1109/EFTF.2012.6502358, pages 163–165, 2012.
10. K. Przemyslaw et al., “Remote Atomic Clock Delivery to the VLBI Station in Torun”, *Proc. of European Frequency and Time Forum 2016*, pages 183, 2016.
11. J. Yang et al., “Development of the Cryogenic 2-14 GHz Eleven Feed System for VLBI2010”, *6th European Conference on Antennas and Propagation*, DOI 10.1109/EuCAP.2012.6206604, pages 621–625, 2011.
12. A. Akgiray et al., “Circular Quadruple-Ridged Flared Horn Achieving Near-Constant Beamwidth Over Multioctave Bandwidth: Design and Measurements”, *IEEE Trans. Antennas Prop.*, 61(3), DOI 10.1109/TAP.2012.2229953, pages 1099–1108, 2013.
13. C. Beaudoin and A. Niell, “Post-correlation Processing for the VLBI2010 Proof-of-concept”, *IVS 2010 General Meeting Proceedings* Edited by Dirk Behrend and Karen D. Baver NASA/CP-2010-215864, pages 35–39, 2010.
14. A. Niell, and Broadband Development Team, “The NASA VLBI2010 Proof-of-concept Demonstration and Future Plans”, *IVS 2010 General Meeting Proceedings* Edited by Dirk Behrend and Karen D. Baver NASA/CP-2010-215864, pages 23–27, 2010.
15. G. Tuccari, “Development of a Digital Base Band Converter (DBBC): Basic Elements and Preliminary Results”, *New Technologies in VLBI*, Asto. Soc. Pacific Conf. Ser. ISSN 1050-3390, Vol. 306, pages 177–252, 2004.



16. H. Takeuchi et al., "Development of a 4 Gbps Multifunctional Very Long Baseline Interferometry Data Acquisition System", *Publ. Astr. Soc. Pacific*, 118, pages 1739–1748, 2006.
17. A. Niell et al., "RDBE Development and Progress", *IVS 2010 General Meeting Proceedings*, Edited by Dirk Behrend and Karen D. Baver NASA/CP-2010-215864, pages 396–399, 2010.
18. B. Petrachenko et al., "Design Aspects of the VLBI2010 System", *Progress Report of the VLBI2010 Committee. NASA Technical Memorandum*, NASA/TM-2009-214180, June 2009.
19. K. Takefuji et al., "High-order Sampling Techniques of Aliased Signals for Very Long Baseline Interferometry", *Publ. Astr. Soc. Pacific*, 124, pages 1105–1112, 2012.
20. T. Oyama et al., "New VLBI Observing System 'OCTAVE-Family' to Support VDIF Specifications with 10 GigaE for VERA, JVN, and Japanese e-VLBI (OCTAVE)", *IVS 2012 General Meeting Proceedings* Edited by Dirk Behrend and Karen D. Baver NASA/CP-2012-217504, pages 91–95,
21. T. A. Clark et al., "Precision Geodesy Using the Mark-III Very-Long-Baseline Interferometer System", *IEEE Trans. Geosci. Remote Sensing*, GE-23(4), IOD 10.1109/TGRS.1985.289433, pages 483–449, 1985.
22. A. E. E. Rogers, "Very long baseline interferometry with large effective bandwidth for phase-delay measurements", *Radio Science*, 5(10), DOI 10.1029/RS005i010p01239, pages 1239–1247, 1970.
23. H. Kiuchi et al., "K-3 AND K-4 VLBI VLBI DATA ACQUISITION TERMINALS", *J. Comm. Res. Lab.*, 38(3), pages 435–457, 1991.
24. T. Kondo and K. Takefuji, "An algorithm of wideband bandwidth synthesis for geodetic VLBI", submitted to *Radio Science*, 2016.
25. Y. Fukuzaki et al., "Construction of a VGOS Station in Japan", *IVS 2014 IVS General Meeting*, Edited by Dirk Behrend, Karen D. Baver, and Kyla L. Armstrong Science Press (Beijing) ISBN 978-7-03-042974-2, pages 32–35, 2014.
26. M. Kimura, "Development of the software correlator for the VERA system II", *IVS NICT-TDC News*, 28, pages 22–25, 2007.
27. A. Saito, S. Fukao, and S. Miyazaki, "High resolution mapping of TEC perturbations with the GSI GPS network over Japan", *Geophys. Res. Lett.*, 25(6), DOI 10.1029/98GL52361, pages 3079–3082, 1998.
28. A. R. Thompson, J. M. Moran, and G. W. Swenson, JR., "Interferometry and Synthesis in Radio Astronomy", KIEGER Pub., Malabar, Florida, ISBN 0-89464-859-4, pages 428–436, 1986.
29. J. W. Armstrong, and R. A. Sramek, "Observations of Tropospheric phase scintillations at 5GHz on vertical path", *Radio Science*, 17(6), DOI:10.1029/RS017i006p01579, pages 1579–1586, 1982.
30. D. Gordon et al., "GSFC VLBI Analysis Center Report", *IVS 2014 Annual Report*, edited by K. D. Baver, D. Behrend, and K. L. Armstrong, NASA/TP-2015-217532, pages 221–224, 2015.